JOC The Journal of Organic Chemistry

Article

pubs.acs.org/joc

On-Demand Cyclophanes: Substituent-Directed Self-Assembling, Folding, and Binding

Pierre-Thomas Skowron,[†] Melissa Dumartin,[‡] Emeric Jeamet,[‡] Florent Perret,[‡] Christophe Gourlaouen,[§] Anne Baudouin,[‡] Bernard Fenet,[‡] Jean-Valère Naubron,[†] Frédéric Fotiadu,[†] Laurent Vial,[∥] and Julien Leclaire*[,‡]

[†]Institut des Sciences Moléculaires de Marseille, UMR 7313 CNRS − Université d'Aix-Marseille − École Centrale Marseille, Avenue Escadrille Normandie-Niemen, 13397 Marseille Cedex 20, France

[‡]Institut de Chimie et Biochimie Moléculaires et Supramoléculaires, UMR 5246 CNRS − Université Claude Bernard Lyon 1 − CPE Lyon, 43 Boulevard du 11 Novembre 1918, 69622 Villeurbanne Cedex, France

[§]Institut de Chimie de Strasbourg, UMR 7177 CNRS − Université de Strasbourg, 1 rue Blaise Pascal, 67008 Strasbourg Cedex, France

[∥]Institut des Biomolécules Max Mousseron, UMR 5247 CNRS − Université de Montpellier, Place Eugène Bataillon, 34296 Montpellier Cedex 5, France

Supporting Information

ABSTRACT: A family of *p*-cyclophanes based on bis- or tetrafunctionalized 1,4-bisthiophenol units linked by disulfide bridges was obtained by self-assembly on a gram scale and without any chromatographic purification. The nature of the functionalities borne by these so-called dyn[4]arenes plays a crucial role on their structural features as well as their molecular recognition abilities. Tuning these functions on demand yields tailored receptors for cations, anions, or zwitterions in organic or aqueous media.

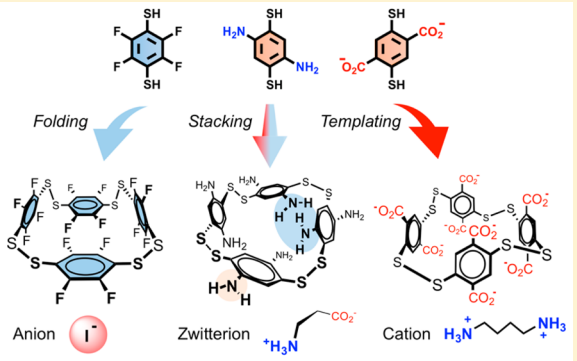

INTRODUCTION

Pedersen's seminal discovery of crown ethers simultaneously brought two cornerstones to the emerging edifice of supramolecular chemistry.[1] These macrocyclic entities were the first nanocontainers with well-defined cavities dedicated to molecular recognition. It also revealed how noncovalent interactions can act as powerful driving forces during covalent self-assembly processes. Since then, supramolecular chemists have learned to produce various cavitands such as calixarenes,[2] pillarenes,[3] cyclodextrins,[4] or cucurbiturils.[5] While these architectures can be obtained at relatively large scale from accessible starting material, a few numbers of templates and functional groups are unfortunately compatible with the generally harsh oligomerization conditions, yielding mixtures that often require tedious chromatographic purifications and postsynthetic functionalization steps, respectively.

During the past 20 years, dynamic combinatorial chemistry (DCC) has emerged as an interesting alternative to produce robust covalent macrocyclic architectures in mild conditions.[6] By operating under thermodynamic control, DCC relies on noncovalent interactions as tunable driving forces to displace equilibrium mixtures in the absence or presence of a molecular partner toward discrete molecular objects in solution or within a condensed phase. Among the available reversible reactions, the disulfide bond exchange, used by Nature to select the optimal structures of proteins for a biological function, is probably one of the most popular given its wide functional group tolerance.[7,8] The disulfide bond exchange reaction occurs spontaneously in aqueous solution at pH values between 7 and 9 and may be quenched by simply lowering the pH. Sanders and colleagues pioneered its use in DCC to produce in aqueous media topologically complex architectures, receptors, and catalysts.[9−11] Yet, such an approach comes with two major drawbacks. First, while expanding the constitutional diversity of the system increases the probability of identification of a hit, it simultaneously hampers the isolation and purification processes. Even from biased libraries, high performance chromatographic tools are required and only modest quantities of the hit can be accessed. The second drawback is inherent to the equilibrium displacement concept: library members of high intrinsic stability combining strong affinity for the target will

Received: November 12, 2015
Published: December 21, 2015

DOI: 10.1021/acs.joc.5b02605
J. Org. Chem. 2016, 81, 654−661

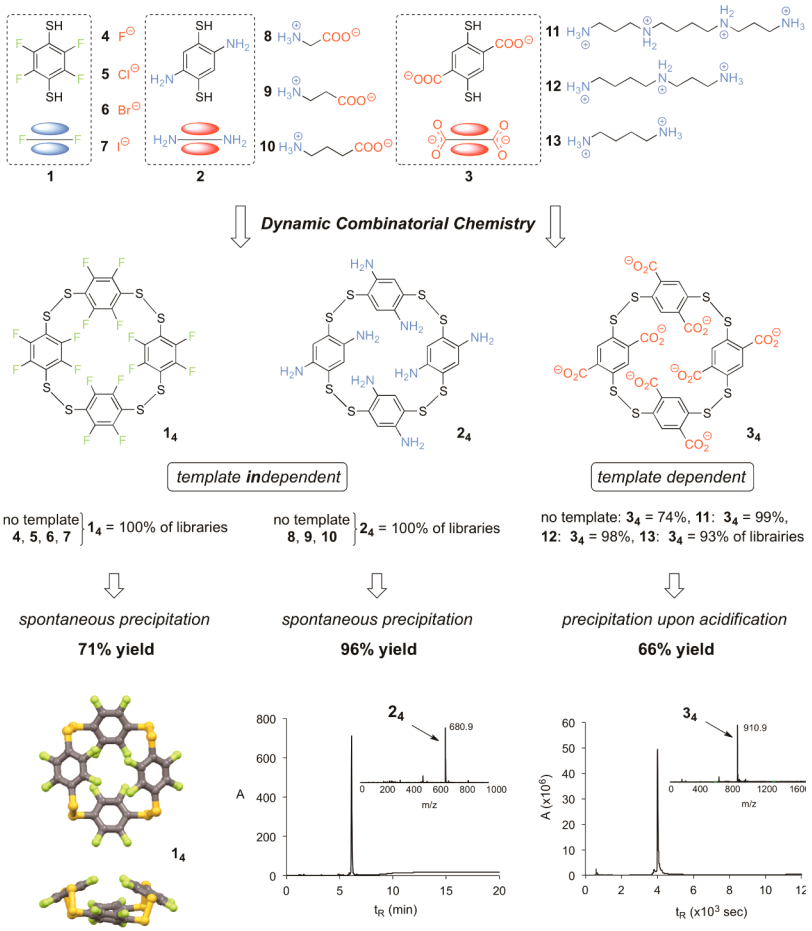

Figure 1. Dynamic combinatorial libraries from bisthiophenols **1**−**3** and templates **4**−**13**, and subsequent isolation of dyn[4]arenes $\mathbf{1}_4$−$\mathbf{3}_4$. Electronic features: red = electron-rich, blue = electron-poor. See Supporting Information for full details.

behave as "false negative" during the dynamic screening process.[12]

By exploring the DCC of 1,4-bisthiophenols, we report herein the easy preparation of a family of *p*-cyclophanes that incorporate dynamic disulfide linkages and various functional groups through quantitative self-assembly. These so-called dyn[4]arenes could be obtained in a gram scale by a straightforward procedure that takes profit of intra- or intermolecular noncovalent driving forces. These forces dramatically depend on the chemical functions borne by the monomers and further determine the structural and binding features of the resulting macrocycles.

RESULTS AND DISCUSSION

Syntheses. A conventional dynamic combinatorial approach was first followed to screen for the best receptors for ionic templates of different polarities from libraries of cyclic homo-oligomers. We investigated the disulfide-based self-assembly of three distinct bis- or tetrafunctionalized 1,4-bisthiophenols **1**−**3** in the absence and in the presence of potential ionic partners **4**−**13** (Figure 1). Substituents were chosen to provide electronically contrasted donor/acceptor sites on monomers **1**, **2**, and **3** to generate dynamic libraries of oligomers that display π-acidic, π-basic combined with H-bond donating/accepting, and π-basic combined with H-bond accepting properties, from which anionic (**4**−**7**), zwitterionic (**8**−**10**), and cationic (**11**−**13**) guests could potentially amplify their optimal receptor, respectively.[13]

Libraries generated from **1** in chloroform invariably and quantitatively yielded a single oligomeric product, which was identical to the adduct obtained by Raasch who hypothesized a cyclic tetrameric structure $\mathbf{1}_4$ from mass spectrometry data (Figure 1).[14] Interestingly, $\mathbf{1}_4$ could also be isolated from a neutral aqueous medium (200 mM Tris buffer, pH 7.4) by simultaneous self-assembly and precipitation (71% yield). A crystal structure was obtained for the first time for this compound, confirming its identity and conformation in the solid state (see Supporting Information for details).

Libraries generated from **2** in the presence or absence of template in Tris buffer (200 mM, pH 7.4) delivered an alternative example of convergence, yielding quantitatively $\mathbf{2}_4$ as a single insoluble species (Figure 1). The identity and purity of the macrocycle was confirmed by HPLC coupled to mass spectrometry, NMR, and elemental analysis.

Libraries generated from **3** surprisingly revealed that fragment polyamines **12** and **13** have almost the same templating effect as the parent spermine **11** previously reported for its quantitative amplification of $\mathbf{3}_4$ (Figure 1).[15] This qualitative deconvolution suggested that the shorter 1,4-diammonium motif already displays all the necessary recognition features that are required to efficiently bind $\mathbf{3}_4$ (vide infra). Unlike the previous macrocycles, $\mathbf{3}_4$ remained soluble in a neutral aqueous medium (200 mM Tris buffer, pH 7.4). Its isolation was simply achieved by precipitation upon

DOI: 10.1021/acs.joc.5b02605
J. Org. Chem. 2016, 81, 654−661

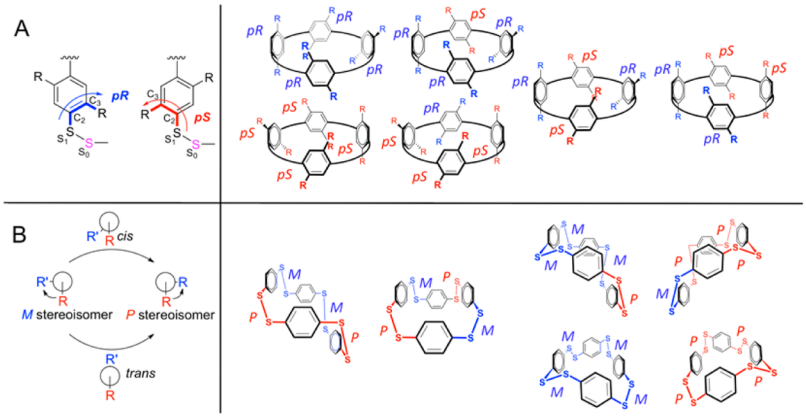

Figure 2. Dyn[4]arene virtual conformational landscape from the rotation of phenyl units (A), and the inversion of the dihedral angle of disulfide bonds (B).

neutralization of its anionic charges with trifluoroacetic acid (66% yield). The identity and purity of the oligomer was again confirmed by HPLC coupled to mass spectrometry and elemental analysis.

Whereas high performance chromatography has been systematically conducted so far for hit isolation from disulfide-based libraries, highly dominant species can clearly be accessed by simpler and more straightforward procedures. Dyn[4]arenes $\mathbf{1}_4$, $\mathbf{2}_4$, and $\mathbf{3}_4$ can be prepared in a gram scale with good yields (66−96%) and excellent purities and without any chromatographic step. We therefore decided to explore the structural features of these macrocycles to elucidate the driving forces underpinning the remarkably efficient self-assembly processes.

Conformational Analyses in Solution. Due to their reduced synthetic accessibility[16,17] and/or low solubility,[18,19] disulfide-based cyclophanes have barely been characterized in solution from a structural point of view. Attention has been drawn to their binding properties, while often considering these objects as members of a structurally and conformationally homogeneous population. Yet, the synthesis of homologous pillar[*n*]arenes is known to yield stereoisomers because the rotation of each of the [*n*] phenyl units along the 1−4 axis leads to structures displaying [*n*] planes of chirality with two opposite *pR*/*pS* configurations (Figure 2A).[20] For dyn[*n*]arenes, a second level of structural diversity arises from the chirality of each of the [*n*] disulfide linkages, which can individually adopt two stabilized enantiomeric *P*/*M* conformations (Figure 2B). We decided to explore the conformational landscape of dyn[4]arenes $\mathbf{1}_4$−$\mathbf{3}_4$ in solution by NMR spectroscopy and DFT calculations.

While the octamethoxydyn[4]arene was described to adopt in the solid state a homochiral *PPPP*/*MMMM* conformation with phenyl groups perpendicular to the average plane of the polydisulfide ring,[20] its perfluoro analogue $\mathbf{1}_4$ crystallizes in a much more flattened conformation. Interestingly, this structural feature survives the dissolution in an organic medium, which indicates that it originates from intramolecular interactions. Indeed, three tetrameric species could be identified on the ^{19}F NMR time scale (Figure 3 and section S3.1).

The two most abundant (87% and 11%) conformers each displayed two sets of signals corresponding to internal (shielded) and external (deshielded) fluorine nuclei in relatively slow mutual exchange (60 kJ mol^{-1}). The exchange is faster for the third minor species (2%), resulting in a single signal in ^{19}F

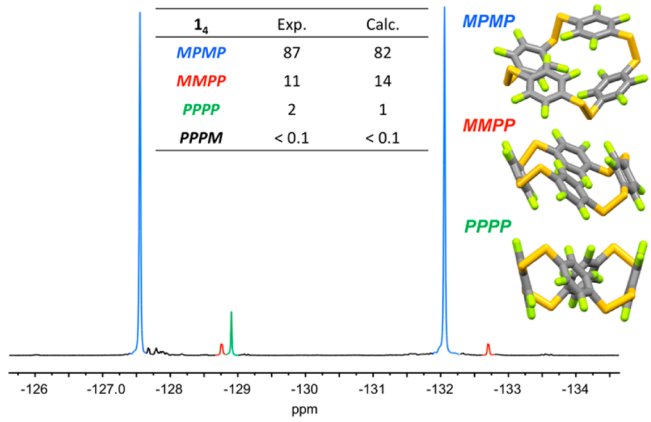

Figure 3. Conformer structure and distribution in solution for dyn[4]arene $\mathbf{1}_4$ from ^{19}F NMR studies in $CDCl_3$ and from DFT calculations. See Supporting Information for full details.

NMR. DFT calculations in solution at the Møller−Plesset second-order perturbation theory level (MP2) are in fair agreement with the experimental data, allowing us to assign these three species to the folded meso *MPMP*, meso *MMPP*, and homochiral *PPPP*/*MMM* conformers, respectively. Although the flattened shape of $\mathbf{1}_4$ could be intuitively attributed to C−F/pi interactions, calculations also revealed that it mostly originates from dispersive forces (see section S4.1).

$\mathbf{2}_4$, which is amplified by self-aggregation, also exemplifies the dramatic impact of the functional groups borne by the monomeric units on the conformational features of the resulting dyn[4]arene. Three types of aromatic protons (Figure 4, H_a, H_b, and H_c) were observed in ^{1}H NMR and appeared to belong to a unique species (see section S3.1.2 for the full multidimensional NMR analysis). Conformational analysis in solution by DFT calculations (at the wB97XD/6-31G(d,p) level, see section S4.2) exclusively yielded species involving an internal N···H−N hydrogen bond between two nonadjacent aromatic units. This internal interaction has two major structural consequences: (i) the monomeric units engaged in this bond are bent into the cavity with amino groups facing each other, and (ii) the homochiral *pRpRpSpR*/*MMMM* and *pSpSpRpS*/*PPPP* enantiomeric dynarenes are the only stable conformers. This internal bond is extremely robust, and coalescence could not be observed upon heating (up to 100

DOI: 10.1021/acs.joc.5b02605
J. Org. Chem. 2016, 81, 654−661

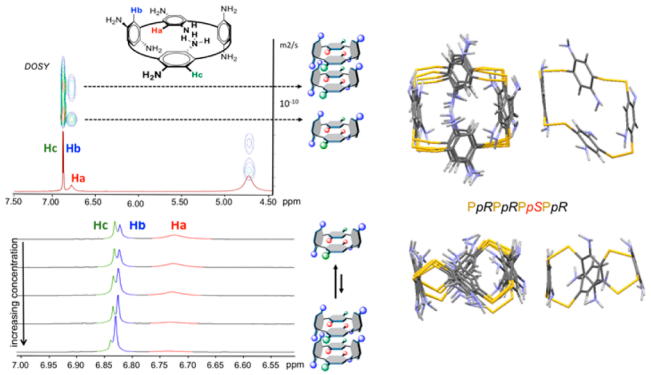

Figure 4. Conformer structure and distribution in solution for dyn[4]arene $\mathbf{2}_4$ from ^{1}H NMR studies in DMSO-d_6 and from DFT calculations. See Supporting Information for full details.

°C). In addition, the two sharp signals H_b and H_c tend to fuse while H_a undergoes severe line broadening upon concentration, suggesting a self-association event in solution. DOSY experiments indeed revealed that two populations of monomeric $\mathbf{2}_4$ and dimeric $\mathbf{2}_4{\cdot}\mathbf{2}_4$, displaying hydrodynamic radii of 8.2 and 15.6 Å, respectively, coexist in solution with concentration-dependent proportions (see section S3.3.3 for details).

Tetramer $\mathbf{3}_4$, which bears anionic monomeric units, was characterized by a single sharp peak in ^{1}H NMR (see section S3.1.3). Our previous modeling study suggested that it corresponds to the cylindrical-shaped homochiral $(pS)_4/(pR)_4$ species, which minimizes the repulsive Coulombic interactions between nearest carboxylate neighbors. This homochiral configuration of the dicarboxyphenyl units in turns directs the disulfide bridges into a homochiral conformation. This analysis agrees with the experimental detection of a unique C−H signal (the kinetic barrier for the inversions of the disulfide bridge's dihedral angle was estimated to be around 75 kJ mol^{-1}, a value that should lead to signal splitting at the NMR time scale if several conformers coexist).

Interestingly, the supramolecular forces that dictate the self-assembly of tetramers $\mathbf{1}_4$, $\mathbf{2}_4$, and $\mathbf{3}_4$, intramolecular stabilization, intermolecular self-stabilization, and templating, respectively, have left a significant conformational imprint on the resulting architectures. These contrasted conformational features, which are dictated by the nature of substituents on the monomeric units, should also substantially affect the binding properties of dynarenes.

Binding Properties in Solution. As initially intended during the preliminary dynamic combinatorial screening, the homo-oligomers combining a π-acidic cavity surrounded by hydrogen accepting sites ($\mathbf{1}_4$), a π-basic cavity surrounded by neutral hydrogen bond donating/accepting sites ($\mathbf{2}_4$), and π-basic cavities surrounded by anionic hydrogen bond accepting sites ($\mathbf{3}_4$) were respectively probed as receptors for anions, zwitterions, and cations. In good agreement with DOSY experiments, molecular modeling revealed that the three dyn[4]arenes have similar diameters and hosting capacities with a maximal cavity diameter of 5.3−6.0 Å (Figure 5), which is comparable to pillar[5]arene, while being much less floppy than their static homologues in terms of phenylene rotation (see Supporting Information section S4.4 and references herein for details). Still, their respective folding states, hence the morphology and accessibility of their potential binding sites, are radically different within the series. Binding properties of dyn[4]arenes in solution were investigated by UV−vis titration in organic media for $\mathbf{1}_4$ and $\mathbf{2}_4$ and by ITC in neutral aqueous media for $\mathbf{3}_4$.

According to its cavity size and π-acidic character, $\mathbf{1}_4$ displayed millimolar affinity for iodide, yielding a 1:1 complex in chloroform accompanied by charge-transfer features (see section S6.2.1). No binding could be detected with the smaller bromide, chloride, and fluoride ions (Figure 5). No modification of the ^{19}F NMR spectrum of $\mathbf{1}_4$ was observed upon iodide addition, which is in agreement with previous reports on anion−pi interactions[21−24] and suggests that the conformational landscape of the host remains unchanged upon guest binding (absence of induced fit). Despite the modest π-acidic character of **1**, a macrocyclic effect,[25] partly relying on the preorganization of $\mathbf{1}_4$, is suggested to explain the selective and efficient binding of iodine in the halogen series through anion−pi interactions.

Dyn[4]arene	$\mathbf{1}_4$	$\mathbf{2}_4$	$\mathbf{3}_4$
Hydrodynamic radius (Å)	8.2[a]	8.2, 15.2 (dimer)[b]	9.2[b]
External radius (Å)	7.4	8.0	8.1
Cavity diameter (Å)	5.3	5.9	6.0
Electrostatic potential surface	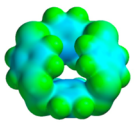	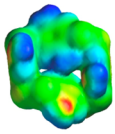	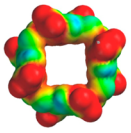
Kd	**4**: no binding[c] **5**: no binding[c] **6**: no binding[c] **7**: 0.3 mM[c]	**8**: no binding[d] **9**: 63 μM[d] **10**: 13 μM[d]	**11**: 6.3 nM[e] **12**: 7.9 nM[e] **13**: 79 nM[e]

Figure 5. Structure−binding relationships for dyn[4]arenes $\mathbf{1}_4$−$\mathbf{3}_4$: hydrodynamic radii from DOSY experiments in $CDCl_3$ (a) and DMSO-d_6 (b); cavity diameters, external diameter, and electrostatic potential surfaces from DFT calculations, and thermodynamic parameters for the binding events with **4**−**13** from UV and ITC titrations in $CHCl_3$ (c), 95% DMSO/5% aq $AcONH_4$ (d), and 40 mM Tris buffer pH 7.4. See Supporting Information for full details.

DOI: 10.1021/acs.joc.5b02605
J. Org. Chem. 2016, 81, 654−661

While $\mathbf{1}_4$ adopts upon self-assembly a tetrahedral shape that leads to a binding site for spherical anions, the cavity of $\mathbf{2}_4$ is entirely occupied by bent hydrogen-bonded monomeric units. As a consequence, the dyn[4]arene displays an electron-poor cleft and an electron-rich area, both sites lying 6 Å away from each other (Figure 5). UV-titrations with substituted α,ω-amino acids in a DMSO/aqueous ammonium acetate mixture revealed that glycine (**8**) is too short to bridge this gap through noncovalent interactions, while both β-alanine (**9**) and γ-aminobutyric acid (GABA, **10**) form 1:1 complexes with submillimolar affinities. No binding was observed with monoanions such as carboxylates or primary ammoniums of various chain lengths in the same conditions. The absence of significant alteration in both the host and guest NMR spectrum upon binding confirms that (i) this binding event follows a lock-and-key scenario, without any induced-fit phenomenon, and (ii) the methylene spacers of the guest remain exposed to the outer solution in the complexes. Because the unfolding of $\mathbf{2}_4$ represents a prohibitive energetic cost, it narrows the spectrum of potential guests to zwitterions that display an appropriate distance between their end groups.

The new synthetic procedure described herein, which provides a straightforward access to substantial amounts of $\mathbf{3}_4$, opens the ways to comprehensive analyses of the complexing features of this type of architecture in aqueous solution for various cationic guests. Butanediamine **13**, spermidine **12**, and spermidine **11** were chosen as models to provide a preliminary insight into the issues that can be addressed through ITC titration and ^{1}H NMR analyses. This modest series formally consists of the successive mutation of one binding N−H proton into an aminopropyl secondary binding group on one or both nitrogens of the butanediamine core. This core remains the main binding site on which the pseudorotaxane structure of the complex is centered as indicated by the almost identical and systematic strong shielding of the corresponding C−H protons in ^{1}H NMR. Whereas substitution on the butanediamine ends only slightly decreases the electrostatic potential of each of these main binding sites (by less than 5% each, data not shown) it could be expected to reinforce the association by providing additional intramolecular cationic binding sites from which some chelate effect may arise. Yet, if the binding is indeed reinforced by 1 order of magnitude, ITC reveals that this increase is entropically driven (Figure 6). This phenomenon can only be imputed to desolvation and confirms that the supplementary binding sites are desolvated upon binding hence involved in complex formation. The evolution in enthalpy reveals that the accompanying desolvation penalty overcomes the benefits of supplementary binding site(s) but that a chelate effect can indeed be observed when comparing spermidine to spermine. Analysis of the ^{1}H NMR spectrum of the complexes (see section S5.2 for details) indicate that enantiotopic methylene protons of the butanediamine thread become clearly diastereotopic upon complexation, confirming the homochiral $(pS)_4$/$(pR)_4$ configuration of the host $\mathbf{3}_4$.[14] Yet, fast exchange between two diastereoisomeric complexes occurs in the case of spermidine (Figure 6b), which result in an average spectrum displaying broad signals for the butanediamine moiety. The loose nature of this complex agrees reasonably well with its increased entropy and reduced enthalpy of formation with respect to parent guests **11** and **13**.

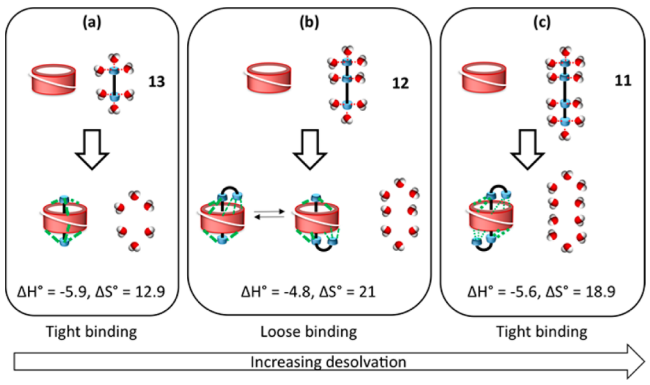

Figure 6. Binding models between $\mathbf{3}_4$ and guest **11**−**13** and associated enthalpy and entropy. $\Delta H°$ and $\Delta S°$ are expressed in kcal·mol^{-1} and cal·mol^{-1}·K^{-1}, respectively. See Supporting Information for full details.

CONCLUSION

The functional group-directed self-assembly of 1,4-bisthiophenol building blocks has led to the gram scale and chromatography-free preparation of a family of *p*-cyclophanes named dynarenes. Beyond the exciting perspectives offered by this new class of highly accessible objects, this preliminary report illustrates the power of the molecular programs contained in simple building blocks. Indeed, the nature of the functionalities borne by the precursors determines the selection event (folding-, aggregation-, or guest-directed) that is responsible for self-assembly. While the conformational landscape of this family is potentially vast, well-structured architectures in solution (tetrahedral, flattened, or cylindrical) result from these function-dependent driving forces. Finally, these structural imprints also dramatically govern the guest binding abilities of dyn[4]arenes by preferentially orienting the association events toward a lock-and-key mode, hence tuning the spectrum of selectivities toward electronically and structurally complementary guests. In the present case, receptors with milli- to submicromolar affinities and selectivities for anions, zwitterions, and cations were obtained. We are currently working toward the expansion of this new family of macrocycles in terms of ring sizes and functionalities for future exciting applications.

EXPERIMENTAL SECTION

Synthesis of the Building Blocks. Building block **1** tetrafluorobenzene-1,4-dithiol):[14] Tetrafluorohydroquinone (4.3 g, 23.63 mmol) was dissolved in 45 mL of anhydrous DMF under argon. At 0 °C, 4 equiv of DABCO (10.62 g, 94.51 mmol) was added, and after 5 min, 4 equiv of dimethylthiocarbamoyl chloride (11.70 g, 94.51 mmol) was added portionwise to the reaction mixture. The suspension was allowed to warm to room temperature and stirred for 1 day. The reaction mixture was poured on ice and filtered, and the residue was washed extensively with water dried under vacuum to give *O*,*O*′-(perfluoro-1,4-phenylene) bis(dimethylcarbamothioate) as a white solid, which was crystallized in acetone to give 8.22 g (yield = 98%) of a white powder. ^{1}H NMR (300 MHz, $CDCl_3$): δ = 3.46 (s, 6H), 3.38 (s, 6H); ^{13}C NMR (75 MHz, $CDCl_3$): δ = 184.8, 140.1, 140.0, 139.8, 44.2, 39.2; ^{19}F NMR (282 MHz, $CDCl_3$): δ = −153.79; HRMS (ESI +): *m*/*z*: calcd for $C_{12}H_{12}N_2O_2S_2F_4Ag^+$: 462.9322 [M + Ag]$^+$; found: 462.9323; mp: 194 °C.

O,*O*′-(Perfluoro-1,4-phenylene) bis(dimethylcarbamothioate) (900 mg, 2.53 mmol) was suspended in 3 mL of diphenyl ether under argon atmosphere and heated on a sand bath to 200−210 °C for 1 h 30 min. The reaction mixture was allowed to slowly cool to room temperature. The reaction mixture was poured on 200 mL of petroleum ether under strong stirring. The resulting precipitate was then filtered, extensively

DOI: 10.1021/acs.joc.5b02605
J. Org. Chem. 2016, 81, 654−661

washed with large amount of petroleum ether, and then dried under vacuum to give 850 mg (yield = 94%) of *S*,*S*′-(perfluoro-1,4-phenylene) bis(dimethylcarbamothioate). ^{1}H NMR (300 MHz, $CDCl_3$): δ = 3.15 (s, 6H), 3.03 (s, 6H); ^{13}C NMR (75 MHz, $CDCl_3$): δ = 161.9, 145.8, 145.7, 145. 6, 37.4; ^{19}F NMR (282 MHz, $CDCl_3$): δ = −131.10; HRMS (ESI+): *m*/*z*: calcd for $C_{12}H_{13}N_2O_2S_2F_4^+$: 357.0349 $[M + H]^+$; found: 357.0350; mp: 237 °C.

S,*S*′-(Perfluoro-1,4-phenylene) bis(dimethylcarbamothioate) was suspended under argon in 3 mL of a 4.2 M degassed solution of KOH in MeOH/H_2O (5/1). The mixture was then refluxed for 1 h 30 min. The reaction mixture was allowed to cool to room temperature, and degassed water (13 mL) was added to the solution followed by HCl (10%, 5 mL) to afford a white precipitate. The precipitate was filtered, washed with degassed water, and dried under vacuum to give tetrafluorobenzene-1,4-dithiol as a white solid (233 mg, 71% yield). ^{1}H NMR (500 MHz, $CDCl_3$): δ = 3.66 (s, 2H); ^{13}C NMR (126 MHz, $CDCl_3$): δ = 143.65, 143.61, 108.43, 108.41; ^{19}F NMR (471 MHz, $CDCl_3$): δ = −136.95; mp: 65−67 °C.

Building block **2** (2,5-diaminobenzene-1,4-dithiol di-(hydrotrifluoroacetate)):[26] Potassium hydroxide (14.87 g; 265.07 mmol) was dissolved in water (18 mL) and degassed under inert atmosphere and cooled to 0 °C with an ice bath. Then **2**·2HCl (5g; 20.39 mmol) was added by portions to the previous solution. The ice bath can be removed, and the reaction mixture was stirred 2 h at room temperature. The precipitated product was collected by filtration, affording a highly air sensitive white solid which was immediately transfer to the next step. To a round-bottom flask was poured water (100 mL) followed by trifluoroacetic acid (23.25g, 203.9 mmol, 15.6 mL), and the solution was cooled at 0 °C. Then the dibasic potassium salt of **2** was dissolved in degassed water (15 mL) and added carefully to the previous solution. The reaction mixture was stirred at room temperature for 2 h. And the water was removed by evaporation. Then the air-sensitive crude solid was dispersed in degassed methanol and rapidly filtered and dried under vacuum to afford compound **2**·2TFA. (7.8 g; yield = 96%)

Building block **3** (2,5-dimercaptoterephthalic acid):[15] To a solution of 2,5-dihydroxyterephthalic acid diethyl ester (10 g, 39 mmol) in 150 mL of DMF was added 4 equiv of neat DABCO (17.6 g, 156 mmol), and after a few minutes 4 equiv of dimethylthiocarbamoyl chloride (19.4 g, 156 mmol) was added. The suspension was allowed to warm to room temperature and was stirred for 24 h. The reaction mixture was poured on a large amount of water, and the resulting 2,5-bis(dimethylthiocarbamoyloxy)terephthalic acid diethyl ester was filtered off and then dried under vacuum to give 16.0 g (yield = 97%) of a white powder. ^{1}H NMR (300 MHz, $CDCl_3$): δ = 7.72 (s, 2H), 4.30 (q, *J* = 7.1 Hz, 4H), 3.45 (s, 6H), 3.39 (s, 6H), 1.33 (t, *J* = 7.1 Hz, 6H); ^{13}C NMR (75 MHz, $CDCl_3$): δ = 187.1, 163.1, 150.6, 128.6, 127.8, 61.7, 43.4, 39.1, 14.2; Mp: 211 °C.

The 2,5-bis(dimethylthiocarbamoyloxy)terephthalic acid diethyl ester (1g, 2.35 mmol) was heated under nitrogen at 230 °C for 1 h. The mixture was then cooled to room temperature, and the product was recrystallized in absolute EtOH to form pale brown crystals. The crystals were filtered off, yielding 2,5-bis(dimethylthiocarbamoyl-sulfanyl)terephthalic acid diethyl ester (900 mg, 90%). ^{1}H NMR (300 MHz, $CDCl_3$): δ = 8.09 (s, 2H), 4.33 (q, *J* = 7.1 Hz, 4H), 3.14 (s, 6H), 3.04 (s, 6H), 1.35 (t, *J* = 7.1 Hz, 6H); ^{13}C NMR (75 MHz, $CDCl_3$): δ = 165.4, 165.3, 138.8, 137.3, 131.0, 61.7, 37.1, 14.2; mp: 140 °C

To 20 mL of a 1.3 M solution of KOH in H_2O/EtOH (1/1) degassed solution was added the 2,5-bis(dimethylthiocarbamoyl-sulfanyl)terephthalic acid diethyl ester (650 mg, 1.51 mmol). The mixture was purged with argon for 15 min and then heated to reflux overnight. The reaction mixture was allowed to cool to room temperature, and concentrated HCl was added to afford a yellow precipitate. The precipitate was filtered, washed with degassed water, and dried under vacuum to give the pure 2,5-dimercaptoterephthalic acid **3** as a yellow solid (310 mg, 88% yield). ^{1}H NMR (300 MHz, DMSO-d_6): δ = 8.06 (s, 2H); ^{13}C NMR (75 MHz, DMSO-d_6): δ = 166.7, 133.2, 130.0; mp: degradation over 387 °C.

Library Preparation and Analyses. Preliminary dynamic combinatorial screening was conducted as follows: 10 mM stock solution of building block (**1**, **2**·2HCl, or **3**) were prepared by dissolution in 200 mM Tris buffer pH = 7.4 in Milli-Q water. In a 2 mL HPLC vial equipped with a stir bar, 400 μL of each of these solutions was mixed with either 400 μL of a 10 mM template solution in the same buffer and 200 μL of buffer solution or 600 μL of buffer solution. Precipitation occurs for libraries involving building block **2** after several hours and **1** after 48 h. After filtration and washing with water and methanol, libraries [**1**] and [**2**] are redissolved in $CDCl_3$ and DMSO-d_6 respectively. Both libraries are analyzed by HPLC-MS and NMR. Templated and untemplated libraries prepared from **1** and **2** lead to HPLC chromatograms and NMR spectra corresponding to pure $\mathbf{1}_4$ and $\mathbf{2}_4$ in each case. For building block **1**, additional libraries were set in $CDCl_3$ (4 mM, 0.2 mM Et_3N) in the absence and presence of 0.25 equiv of template and lead to identical ^{19}F spectra corresponding to pure tetramer $\mathbf{1}_4$. Additional libraries made from building block **2**·HCl in DMSO (4 mM, 4.2 mM Et_3N) led to side products involving overoxidized sulfur atoms. Libraries [**3**] were analyzed by HPLC-MS.

Oligomer Identification/Quantification. Identification and quantification of the oligomers and potential side products were conducted by HPLC with a heated column compartment (35 °C), and a triple quadrupole mass spectrometer. Mass spectra (ESI−/ESI+) were acquired in ultrascan mode by using a drying temperature of 400 °C, a drying gas flow of 11 L/min, and a capillary voltage of 3000 V (ESI+) or 2000 V (ESI−). Elution was conducted at 1.2 mL/min on a C8 column, 4.6 × 150 mm, 3 μm column (T = 35 °C).

Synthesis of the Macrocycles. *Dyn[4]arene* $\mathbf{1}_4$. A 932 mg amount of **1** was dissolved into 900 mL in 200 mM Tris buffer pH = 7.4. The reaction mixture was stirred for 72 h. The resulting precipitate was then filtered, washed with degassed methanol, and dried under vacuum to give a pale yellow solid (656 mg, 71% yield). Crystal suitable for X-ray analyses were obtained upon recrystallization in chloroform−methanol. ^{19}F NMR (471 MHz, $CDCl_3$): δ = 128.1 (s, *MPMP*), −129.1 (s, *MMPP*), −129.3 (s, *MMMM* + *PPPP*), −132.2 (*MPMP*), −133.0 (s, *MMPP*); ^{13}C NMR (126 MHz, $CDCl_3$): 119.0, 147; HRMS (ESI−): *m*/*z*: calcd for $C_{24}F_{16}S_8$ = 882.7204 $[M + Cl]^-$, found = 882.7238; mp: 248−251 °C (decomp); IR (ATR, cm^{-1}) = 538 (S−S) ; 1250 (C−F) 1464 (C═C), 1618 (C═C).

Dyn[4]arene $\mathbf{2}_4$. A 980 mg (3.84 mmol) amount of **2**·2HCl was dissolved into 1 L of a 200 mM Tris buffer solution adjusted to pH = 8. The reaction mixture stirred for 72 h. The resulting solid was filtered off and then dried under vacuum. A Soxhlet extractor was used overnight to wash the solid with warm methanol. The solid was then dried under vacuum to give 630 mg (yield = 96%) of a dark red powder. The same result was obtained from the bis-(hydrotrifluoroacetate) salt **2**·2TFA, confirming that the anion is not involved in the self-assembling process. ^{1}H NMR (400 MHz, DMSO-d_6): δ = 6.73 (sl, 4H, Ha), 6.83 (s, 2H, Hb), 6.84 (s, 2H, Hc); ^{13}C NMR (126 MHz, DMSO-d_6): δ = 119.3, 121.7, 140.1; HRMS (MALDI): *m*/*z*: calcd for $C_{24}H_{24}N_8S_8^+$ = 679.9884 $[M^{+\bullet}]$, found = 679.9896; Elemental analysis: calcd for $C_{24}H_{24}N_8S_8H_2O$ = C: 41.23, H: 3.75, N: 16.03, S: 37.70; found = C: 41.02, H: 3.42, N: 15.61, S: 37.22; mp: ≈ 200 °C (decomp); IR (ATR, cm^{-1}): 3373 (NH), 1587 (C═C), 1217 (C−N), 875 (CH).

Dyn[4]arene $\mathbf{3}_4$. A 920 mg (4 mmol) amount of monomer **3** was dissolved into 400 mL of a 200 mM Tris buffer pH = 7.4 in the presence of spermine (910 mg, 4 mmol). The reaction mixture was stirred open to the air. After 48 h, a few milliliters of TFA was added and a fine yellow precipitate appeared. The resulting solid was filtered off and taken up in a pH = 9 borate buffer, and then TFA was added. The precipitate was collected by centrifugation, suspended in Milli-Q water, collected by centrifugation again, and then dried under vacuum overnight to give 600 mg (0.66 mmol; 66%) of a yellow powder. ^{1}H NMR (500 MHz, DMSO): δ = 8.29 (s, 1H); ^{13}C NMR (126 MHz, DMSO): δ = 166.95, 137.18, 132.41, 128.93; HRMS (ESI−): *m*/*z*: calcd for $C_{32}H_{15}O_{16}S_8^-$ = 910.8131 $[M - H]^-$, found = 910.8166; Elemental analysis: calcd for $C_{32}H_{15}O_{16}S_8{\cdot}5H_2O$ = C: 38.3 H: 2.61 O: 33.5; S: 25.6; found = C: 36.8; H: 2.67; O: 34.8; S: 25.8; mp: 350 °C

DOI: 10.1021/acs.joc.5b02605
J. Org. Chem. 2016, 81, 654−661

(decomp); IR (ATR, cm^{-1}) = 2887 (OH), 1678 (C═O), 1583 (C═C), 1213 (C−O), 779 (CH).

NMR Studies. Liquid-state NMR spectra were recorded in $CDCl_3$, DMSO-d_6, methanol-d_4, and heavy water buffered with $CD_3CO_2ND_4$ or KD_2PO_4−NaOD on spectrometers operating at 300, 400, and 500 MHz. Solvent residual signals were used as internal standard (when necessary, water suppression by presaturation was used). The temperature was set to 22° C unless otherwise specified. A 2s relaxation time allowed proton full relaxation. ^{13}C spectra were recorded using a 30° tilt angle and 2s relaxation time. ROESY experiments were run using the 2D off-resonance version, with adiabatic trapezoidal 200 ms shape pulse, at 10 kHz field strength. A total of 256 increments of 8 scans were collected giving 1 h 30 min experiment time. Solid-state NMR spectra were recorded on a 9.4 T spectrometer.

Computational Details. Geometry optimizations were conducted at the MP2 level of theory with the DEF2-SVP basis set. Solvent corrections (dichloromethane) were included through the COSMO model. Weak interactions in the system were investigated by means of Non Covalent Interactions (NCI) analysis on the basis of the theoretically optimized geometry.

Dyn[4]arene $\mathbf{1_4}$. The structures of the four conformers of $\mathbf{1_4}$ (namely *PPPP*, *PPPM*, *MMPP*, and *MPMP*) were optimized with solvent corrections. The most stable structure was found to correspond to the *MPMP* conformer. The *MMPP* and *PPPP* structures are slightly less stable, with energies higher by 1.0 and 1.8 kcal·mol^{-1}, respectively. The less stable conformer is the PPPM structure, whose energy is 4.6 kcal·mol^{-1} higher than for the *MPMP*. This scheme is consistent with the abundance found by NMR analysis, with one major compound (around 85%) and two minor species (15% total). The compact structure observed in the crystalline state was retrieved from the calculation in solution. NCI analysis was performed to understand the origin of such folded structure on the four conformers (Figure S46). A network of interaction favoring the compact structures can be clearly observed. They are of two main types. Fluorine atoms of different phenyl moieties clearly interact with each other through weak dispersive forces. An electrostatic interaction can be observed between one fluorine atom and the carbon of the opposite phenyl ring: one C−F fragment can thereby interact with another F−C of the opposite monomer. This interaction accounts for the lower stability of the *PPPM* structure, as this network is partially broken in such a conformation, as it can be seen in Figure S46.

Dyn[4]arene $\mathbf{2_4}$. The conformational study of $\mathbf{2_4}$ was performed using a stochastic exploration of the potential energy surface (PES) using simulated annealing with AM1 semiempirical level. A set of 100 geometries of conformations were generated using four simulated annealings, each performed with a different geometry or parametrized with a different initial temperature. All annealings were performed with a geometry optimized with WB97XD/6-31G(d,p) as the starting structure. Only the dihedral angles of the initial structure were allowed to relax during the annealing; the bonds lengths and the valences angles were kept constant. Then the conformations with energy down to 2.5 kcal mol^{-1}, compared to the lower energy conformation, were kept and fully optimized. The geometry optimizations, vibrational frequencies, and IR absorption intensities were calculated with Density Functional Theory (DFT) using WB97XD functional combined with 6-31G(d,p) basis set.

Dyn[4]arene $\mathbf{3_4}$. Previous modeling conducted by us revealed that the most stable conformation of $\mathbf{3_4}$ corresponds to the cylindrical-shaped homochiral $(pS)_4/(pR)_4$ species, which allows minimization of the repulsive Coulombic interactions between nearest carboxylate neighbors.[15]

Host−Guest Binding. Isothermal titration calorimetry (ITC) experiments were performed at 298 K. In a standard experiment, the host solution (~0.01 mM) in Tris buffer pH 7.4 (200 mM) was placed into the calorimeter cell (200 μL) and 20 successive aliquots (2 μL) of guest solution (10 times more concentrated) were added via a computer-automated injector at 2 min intervals. Heat changes were recorded after each addition. Heats of dilution were subtracted from the titration data prior to curve fitting. The first injection was discarded from each data set to remove the effect of guest diffusion across the syringe tip during the equilibration process.

UV/vis titration experiments were performed at 298 K. All measurements have been run at least in triplicate. All spectra were carried out in quartz UV cuvettes (l = 1 cm). Spectroscopic grade solvents (chloroform, DMSO, Milli-Q water) and analytical grade salts ($AcONH_4$, nBu_4NPF_6). $AcONH_4$ was used to buffer the aqueous DMSO solution and ensure a constant ionic strength protonation state of the amino acid guests used. Similarly, anion−pi interactions between $\mathbf{1_4}$ and anionic guests were probed both in the presence and absence of nBu_4NPF_6 to rule out any solvatochromic effect.

■ ASSOCIATED CONTENT

Supporting Information

The Supporting Information is available free of charge on the ACS Publications website at DOI: 10.1021/acs.joc.5b02605.

Material and methods, HPLC chromatograms, NMR spectra, and MS spectra (PDF)

X-ray crystallographic data (CIF)

■ AUTHOR INFORMATION

Corresponding Author

*E-mail: julien.leclaire@univ-lyon1.fr.

Author Contributions

J.L., L.V., F.P., and F.F. conceived the experiments. P.-T.S, M.D., E.J., F.P., and J.L. performed the experiments. E.J., C.G., and J.-V.N. performed the theoretical analyses. A.B. and B.F. designed and performed the NMR analyses. J.L., F.P., and L.V. analyzed the experimental data and cowrote the paper.

Notes

The authors declare no competing financial interest.

■ ACKNOWLEDGMENTS

This work was supported by the LABEX iMUST (ANR-10-LABX-0064) of Université de Lyon, within the program "Investissements d'Avenir" (ANR-11-IDEX-0007) operated by the French National Research Agency (ANR) (fellowship for E.J. and starting grant for J.L.). We are grateful to the CNRS and ANRT for funding (fellowship for M.D. and P.-T.S. respectively)

■ REFERENCES

(1) Pedersen, C. J. *J. Am. Chem. Soc.* **1967**, *89*, 7017.

(2) Gutsche, C. D. *Calixarenes: An Introduction*, 2nd ed.; Royal Society of Chemistry: Cambridge, 2008.

(3) (a) Xue, M.; Yang, Y.; Chi, X.; Zhang, Z.; Huang, F. *Acc. Chem. Res.* **2012**, *45*, 1294. (b) Cao, D.; Kou, Y.; Liang, J.; Chen, Z.; Wang, L.; Meier, H. *Angew. Chem., Int. Ed.* **2009**, *48*, 9721.

(4) Dodziuk, H., Ed. *Cyclodextrins and Their Complexes: Chemistry, Analytical Methods, Applications*; Wiley: New York, 2006.

(5) (a) Das, D.; Scherman, O. A. *Isr. J. Chem.* **2011**, *51*, 537. (b) Lagona, J.; Mukhopadhyay, P.; Chakrabarti, S.; Isaacs, L. *Angew. Chem., Int. Ed.* **2005**, *44*, 4844.

(6) Corbett, P. T.; Leclaire, J.; Vial, L.; West, K.; Wietor, J.-L.; Sanders, J. K. M.; Otto, S. *Chem. Rev.* **2006**, *106*, 3652.

(7) Otto, S.; Furlan, R. L. E.; Sanders, J. K. M. *J. Am. Chem. Soc.* **2000**, *122*, 12063.

(8) Bang, E.-K.; Lista, M.; Sforazzini, G.; Sakai, N.; Matile, S. *Chem. Sci.* **2012**, *3*, 1752.

(9) Ponnuswamy, N.; Cougnon, F. B. L.; Clough, J. M.; Pantoş, G. D.; Sanders, J. K. M. *Science* **2012**, *338*, 783.

(10) Otto, S.; Furlan, R. L. E.; Sanders, J. K. M. *Science* **2002**, *297*, 590.

(11) Brisig, B.; Sanders, J. K. M.; Otto, S. *Angew. Chem., Int. Ed.* **2003**, *42*, 1270.

DOI: 10.1021/acs.joc.5b02605
J. Org. Chem. 2016, 81, 654−661

(12) Corbett, P. T.; Sanders, J. K. M.; Otto, S. *Chem. - Eur. J.* **2008**, *14*, 2153.
(13) Hunter, C. A. *Angew. Chem., Int. Ed.* **2004**, *43*, 5310.
(14) Raasch, M. S. *J. Org. Chem.* **1979**, *44*, 2629.
(15) Vial, L.; Ludlow, R. F.; Leclaire, J.; Pérez-Fernández, R.; Otto, S. *J. Am. Chem. Soc.* **2006**, *128*, 10253.
(16) Kobayashi, K.; Koyama, E.; Kono, C.; Namatame, K.; Nakamura, K.; Furukawa, N. *J. Org. Chem.* **2001**, *66*, 2085.
(17) Sonawane, P. M.; Jacobs, J.; Thomas, J.; Van Meervelt, L.; Dehaen, W. *Chem. Commun.* **2013**, *49*, 6310.
(18) Wong, D. T-M.; Marvel, C. S. *J. Polym. Sci., Polym. Chem. Ed.* **1976**, *14*, 1637.
(19) Liang, Z. A.; Meng, Y. Z.; Li, L.; Du, X. S.; Hay, A. S. *Macromolecules* **2004**, *37*, 5837.
(20) Zhang, Z.; Luo, Y.; Xia, B.; Han, C.; Yu, Y.; Chen, X.; Huang, F. *Chem. Commun.* **2011**, *47*, 2417.
(21) Jentzsch, A. V.; Emery, D.; Mareda, J.; Metrangolo, P.; Resnati, G.; Matile, S. *Angew. Chem., Int. Ed.* **2011**, *50*, 11675.
(22) Jentzsch, A. V.; Hennig, A.; Mareda, J.; Matile, S. *Acc. Chem. Res.* **2013**, *46*, 2791.
(23) Chifotides, H. T.; Dunbar, K. R. *Acc. Chem. Res.* **2013**, *46*, 894.
(24) Ballester, P. *Acc. Chem. Res.* **2013**, *46*, 874.
(25) Steed, J. W.; Turner, D. R.; Wallace, K., Eds. *Core Concepts in Supramolecular Chemistry and Nanochemistry*; Wiley: New York, 2007.
(26) Wolfe, J. F.; Loo, B. H.; Arnold, F. E. *Macromolecules* **1981**, *14*, 915−920.

DOI: 10.1021/acs.joc.5b02605
J. Org. Chem. 2016, 81, 654−661